Structural and morphological study of nanostructured n-type silicon

Hasan A. Hadi [1], Nadir F. Habubi[1], Raid A. Ismail[2]

[1] Education Faculty, University of Al-Mustansiriyah

[2]Department of Applied Sciences, University of Technology

Abstract

In this study, investigations of structural properties of n-type porous silicon prepared by laser assisted-electrochemical etching were demonstrated. The Photo- electrochemical Etching technique, (PEC) was used to produce porous silicon for n-type with orientation of (111). X-ray diffraction studies showed distinct variations between the fresh silicon surface and the synthesized porous silicon surfaces. Atomic force microscopy (AFM) analysis was used to study the morphology of porous silicon layer. AFM results showed that root mean square (RMS) of roughness and the grain size of porous silicon decreased as etching current density increased. The chemical bonding and structure were investigated by using fourier transformation infrared spectroscopy (FTIR). Porosity of the porous silicon layer and thickness were determined gravimetrically. Increasing the etching current density led to increase the surface porosity and thickness. Porosity between77% and 82% were observed for current densities between 24 mA/cm^2 and 116 mA/cm^2.

Key words

Nano-crystal,
porous silicon,
Photo-chemical etching (PCE).

Article info
Received: Nov. 2011
Accepted: Sep. 2012
Published: Oct. 2012

دراسة الخصائص التركيبية النانوية للسيليكون المسامي من النوع المانح

حسن عبد الصاحب هادي[1] ، نادر فاضل حبوبي[1] ، رائد عبدالوهاب اسماعيل[2]

[1] كلية التربية ، الجامعة المستنصرية

[2] قسم العلوم التطبيقية، الجامعة التكنولوجية

الخلاصة

لقد تم في هذا البحث دراسة الخصائص التركيبية لطبقة السيليكون المسامي على القواعد السيليكونية من النوع المانح المحضر بطريقة التنميش الكهروكيميائي بمساعدة اشعة الليزر .لقد اوضحت نتائج حيود الاشعة السينية XRD ان طيف التركيب المسامي يختلف عن نظيره البلوري. تم استخدام تقنية مجهر القوة الذرية(AFM) لدراسة طبوغرافية السليكون المسامي . لقد اوضحت النتائج العملية ان مقدار الجذر التربيعي لمعدل خشونه سطح السليكون قد ازداد مع زيادة كثافة تيار التنميش. ان التركيب والتأصر الكميائي للسليكون المسامي تم فحصه بواسطة تقنية FTIR . ان النسبة المئوية للمسامية وسمك الطبقة المسامية تم تحديدها بالطريقة الوزنية . لقد وجد ان كل من سمك الطبقة المسامية والنسبة المئوية للمسامية قد ازدادت مع زيادة كثافة تيار التنميش. ان قيم المسامية للطبقة المقاسة بالطريقة الوزنية تزداد من 77% الى 82% عندما يكون كثافة تيار التنميش مابين $24mA/cm^2$ و $116mA/cm^2$.

Introduction

The properties of porous silicon structures are of increased importance for a fundamental understanding of nano systems as well as from a practical point of view to understand and control the materials fabrication processes [1]. The physical properties of porous silicon (PS) are fundamentally determined by the shape and diameter of pores, voids thickness, the relative content of Si. These parameters depend on preparation conditions, so that it is possible to design materials with physical properties of those between Si and air (or the medium which fills the pores) [2].

In recent years, PS has become an increasingly important and versatile electronic material. It's reactive, porous and highly insulating nature allows for the selective formation of unique electronic components and mechanical nanostructures. Despite extensive research on the synthesis of porous semiconductors, the development of regular porous structure with high quality and large surface area remains a key issue for the development of future optoelectronic at nano scale [3]. PS has been widely studied since the early 1990's, due primarily to interest in its development as an efficient light emitting material for optoelectronic applications [4], but A. Prasad et al had been applied to solar cell research as early as 1982[5]. The light trapping and anti-reflection properties of PS, in addition to its simplicity of formation and broadly tunable morphology, make it particularly well suited for photovoltaic applications. In this study, we have synthesized porous silicon surface by photo-electrochemical etching and studied their morphological and structural properties.

Experimental techniques and Preparation Samples.

The fabrication of Porous Silicon (PS) is a comparatively simple process that only requires a small amount of equipment. The simplest cell which can be used to anodize silicon is shown in Fig. 1.

The silicon wafer serves as the anode. The cathode is made of platinum or any HF-resistant and conducting material.

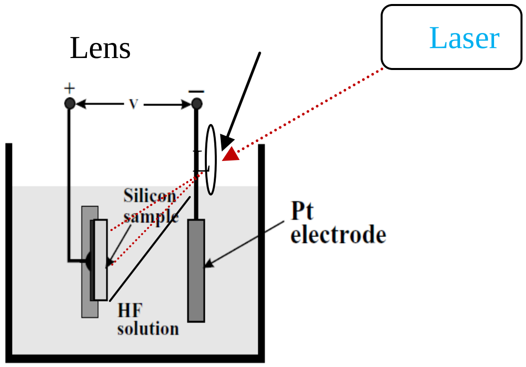

Fig.1:* *Schematic of the designed for fabrication porous silicon.

The diode laser 650nm (10 -40mW) in this case by illuminating n-type substrates surface of the wafer with sufficiently energetic photons; holes can be photo generated in the bulk [6]. In the experiments, Porous silicon films were produced using monocrystalline silicon wafers n-type, with resistivity's10 Ω.cm. The wafers with (111) face orientation. Samples were made of porous silicon produced with a standard technique of anodizing nc-si silicon substrates in an electrolyte HF (40%):(99.8) % CH_3OH with a volume ratio of [1:1]. The Si wafer first had to be diced $1\times1cm^2$ (and smaller than for porosity) samples before cleaning. Cleaning is vital to remove particulate matter as well as any traces of organic, metallic and ionic contaminants from samples. Methanol and alcohol are used commonly clean the wafer by immersing it in these chemicals in turn in the ultrasonic bath for few minutes. Finally, they were rinsed in distilled water treated ultrasonically followed by drying in a hot air stream. Back side of the samples was coated with ~800nm Aluminums layer. The evaporation is performed in a vacuum pressure of 10^{-6} torr, using an evaporation plant model "E306 A manufactured by Edwards high vacuum".Porous silicon (PS) samples were prepared by anodization in $HF:CH_3OH$ (1:1) solution at a constant current density 20 - 60 mA/cm^2 at 10 min.

In this work, an AA 3000 Scanning Probe Microscope AFM system in School of applied sciences, University of Technology has been used. The XRD (shimadzu -6000) system was used for x-ray diffraction measurements. They were then placed into the x-ray (Cu Kα1 line λ = 1.5406 A) generating chamber under acceleration voltage of 40 kV and a current of 30 mA. The sample was scanned from 25 to 40 degrees 2Theta. This measurement is achieved in the National Center for Construction Laboratories and Researches.

Results and Discussion

1. FTIR Measurement

The FTIR spectrum from PS layer is very strong and easier to measure than that from bulk silicon due to the large specific area [7]. The chemical properties of freshly etched silicon samples are very sensitive to surrounding ambient, where it varies with time during storage in air [8], since the pore surface includes a high density of dangling bonds of silicon for original impurities such as hydrogen and fluorine which are residuals from the electrolyte.

From FTIR data Fig. 2 on PS (n-type Si), obtained within 10 minutes after its anodization is completed, it is clear that there are three distinct peaks with different intensities. The peak with intensity at 1080/cm that indicates the presence of Si-O-Si wagging. A small peak at 624/cm can be associated with the Si-H Waggener mode. While a peak at 2854/cm is suggestive of the CH stretching. The changes of chemical bonds due to oxidation can be investigated by FTIR technique. Anodization at 40 mA in 40% methanoic HF [1:1], for 10 min, thermally oxidized in air (at 300 °C for 30 min) are shown in fig (2-a) for n-type. Fig.2-a shows IR absorption spectrum of the PS/Si sample at room temperature, a strong broad band is observed at about 1080cm^{-1} due to Si-O-Si asymmetry stretching absorption bands centered at about 624cm^{-1} are attributed to the wagging modes of the SiH$_x$ species. Absorption at 2854cm^{-1} and 2924cm^{-1} is due to the in plane C–H angle deformation [9]. It can easily replace a silicon atom, leading to the presence of carbon in the porous structure, since carbon is located in the same column of the periodic Table as silicon, [9]. Annealing this surface above 300C promotes hydroxyl conversion into Si-O-Si bridges and produces a partially oxidized porous silicon surface.

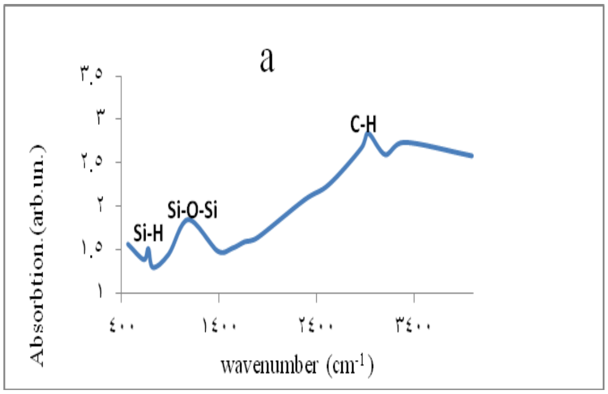

Fig.2-a: FTIR spectrum of the PS layer.

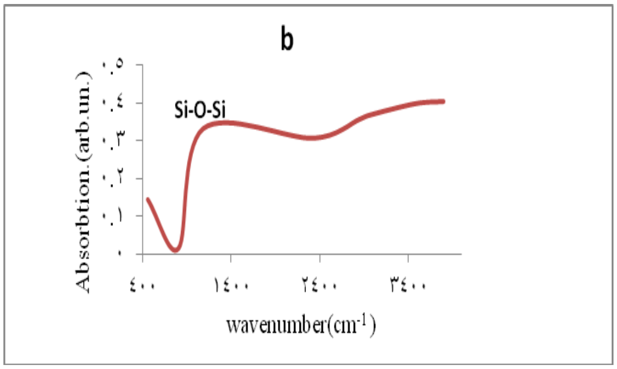

Fig.2-b: FTIR spectrum of the PS layer after oxidized at 300 C for 30 min

Upon annealing in air, new chemical bonds appear on the surface as a wide absorption band due to different Si-H and Si-O chemical bond configurations in the IR spectra. Another notable that if a molecule is so symmetrical that the stretching of a bond does not produce any change in dipole moment, then no IR peak will be found in the spectrum[10]. The (Shimadzu-

IRAffinity-1) scans of the FTIR measurements are performed over range between (400-4000) cm^{-1} for prepared sample. Surface chemical composition of samples is best probed with Fourier Transform Infrared (FTIR) spectroscopy.

Table 1: The chemical bonds found in porous silicon

Functional group	Frequency cm^{-1}	Bonds	Vibration mode	Reference
Si H	624-650	Si-H	Wagging modes	12
Si-O-Si	1080	Si-O-Si	Asymmetry stretch	12
CH	2854	C-H	Asymmetric Stretch.(CH)	12

2. Porosity and Thickness

Porosity and thickness of the nanocrystalline porous silicon layer are very sensitive to many experimental variables, such as the doping density of the silicon substrate, the current density and the etching time. In Fig.3 we can observe that the porosity increases exponentially with the increasing current density. Porosity and thickness of the nanocrystalline porous silicon layer are very sensitive to many experimental variables, such as the doping density of the silicon substrate, the current density and the etching time [11, 12]. It is necessary to determine porosity. The porosity (*P*) is defined as the fraction of voids (air) within the nanocrystalline porous layer. This parameter could be estimated by gravimetric as described in [13]

$$p = \frac{m_1 - m_2}{m_1 - m_3} \% \qquad (1)$$

where m_1 is the silicon mass before etching, m_2 is the mass of the silicon substrate after etching (including porous silicon), and m_3 is the weight the wafer silicon after nano porous silicon removed with NaOH.

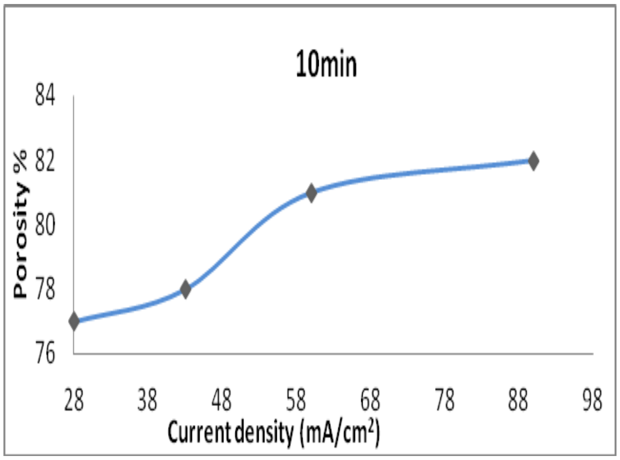

Fig.3: Porosity as a function of current density for n-type porous silicon.

which shows the porosity produced by removed or dissolved silicon mass during the etching divided by the total mass of etched silicon . In the same way, the film thickness of the nanocrystalline porous silicon layer can be estimated by [13].

$$T = \frac{(m_1 - m_3)}{s \times d} \qquad (2)$$

Where d is silicon density (d=2328 mg/cm^3) and S is etched surface as shown in this relation [13]. As shown in figure (3) presence of two regions are evident. In the first region, (1) can observe that the porosity increases (non linear) with the current density (more evident for the n-Si substrates) and then increases linearly with increasing iodization current density in region two. For n-type the porosity varies between 77 and 82% for current densities between 28 and 116 $mAcm^{-2}$. These results presented are agreement with those published by other authors [14- 17]. Where by increasing the current the porosity increases too for a fixed HF concentration as shown in Fig.3, which means that the pore distance decreases as shown later in Table2. Since the porosity (ratio of voids to crystallites) of the PS layer depends on the effective distribution of the voids fractions in the resulting silicon crystallites in the PS matrix, a variation of current density (for other etching parameters such as concentration of the electrolyte, etching time and surface doping of the Si' substrate) can alter the porosity of the sample, thereby depends the refractive index [5,18]. A lateral spatial variation of the porosity is observed for PS layers formed on the Si surface.

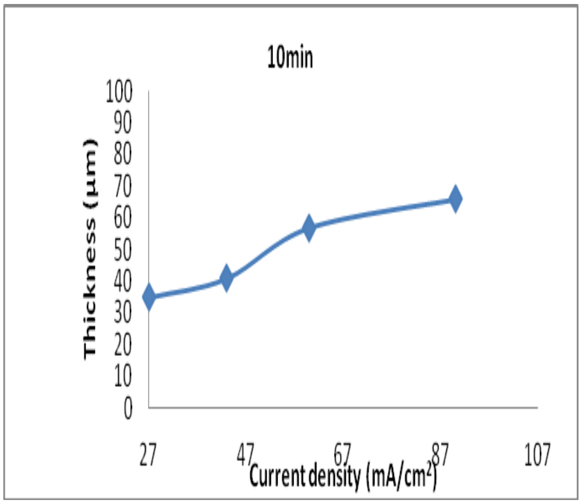

Fig.4: Porous thickness as a function of current density for n-type

The thickness of the layer increases linearly with increase in current densityfrom 27 to 44 mA/cm^2, as shown in Fig.4. The thickness of the PS 1ayers was 35 - 66 µm. Also Fig.4 illustrates that the formation rate of the PS layer rises exponential at J then increase linearity at high current density more than 60mA/cm^2. The microstructure and there by the porosity and the thickness of the PS layer can be controlled by changing various anodization parameters such as current density, etching time….etc.

3. Topological AFM characterization

AFM measurements show that the surface of the etched PS layer consists of a matrix of randomly distributed nanocrystalline Si pillars and voids. The surface morphology measured by AFM is given in Fig.5 which shows that the surface of the PS layer consists of inhomogeneous and large number of irregularly shaped ‘pores and voids’ distributed randomly over the entire surface. Fig.5 (a-b) show the morphology of the porous silicon for photochemical etching anodization process of monocrystalline silicon in HF based solution at 40 and 60mAcm^{-2} for 10 min. Representative 2 µm x 2 µm images 2 and 3 dimension of porous silicon. Root-mean-square (RMS) surface roughness is a commonly accepted parameter to describe surface. It is typically used to quantify variations in surface elevation, the RMS (root mean square) roughness for PS was found to be 5.5-34.4 nm and Sz. (Ten Point height) 41.5-46 nm with large irregular upright structure of silicon crystallites. A change of microstructure of the porous silicon surface were observed for different current density (40 and 60mAcm^{-2}) where pore sizes varied significantly as shown in the AFM picture given in Fig.5 at constant J current density. This roughness is expected to be caused by inhomogeneous of the substrate and electrolyte composition, and seems to increase with layer thickness.

5. X-ray measurement

From the figure shown high peak at $2\theta = 29.38^{o}$, which corresponds to the (111) plane of bulk Si and showing the single crystalline nature of the wafer. This peak becomes very broad with varying full-width at half maximum (FWHM) for different time anodization as shown in Fig.6, which confirms the formation of pores on the crystalline silicon surface. The broadening of a single diffraction peak is the product of the crystallite dimensions in the direction perpendicular to the planes that produced the diffractionpeak.

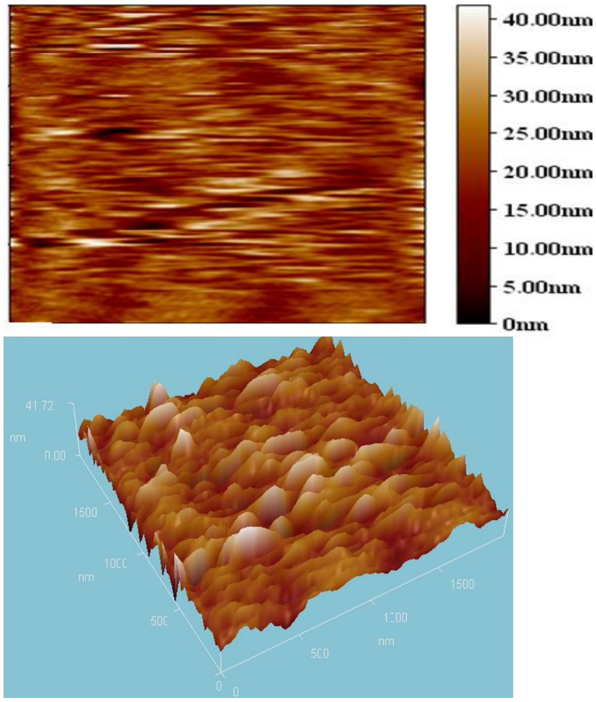

Fig.5-a: 2D and 3D AFM images of PS surface at constant etching time 10 min and at 40Ma/cm^2 etching current density for n-type(2µm×2µm).

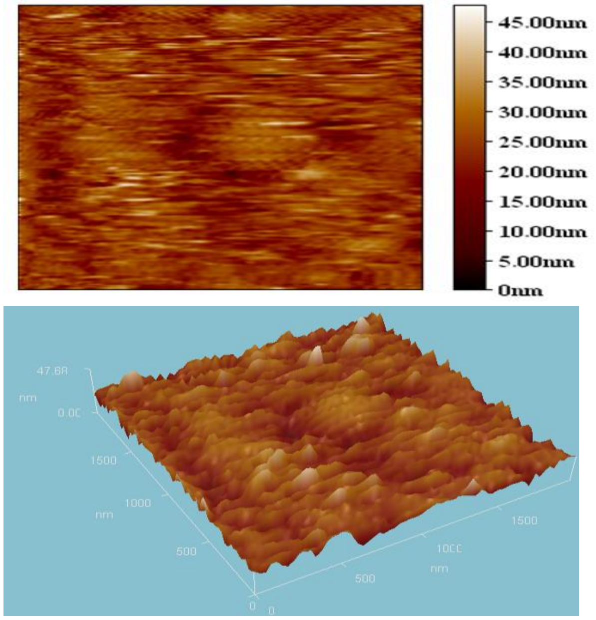

Fig.5-b: 2D and 3D AFM images of PS surface at constant etching time 10 min and at 60Ma/cm^2 etching current density for n-type(2µm×2µm).

However, for etching time 10 min XRD curve show peaks at 2θ = 28.86º and the same plane reflection (111). The broadening in the XRD spectrum may due to the size distributions of pore walls, and upward shifts is due to relaxation of strain in the porous structure. This peak becomes broad with varying full-width at half maximum (FWHM) after (10 min) time anodization as shown in Fig.6, which confirms the formation of pores on the crystalline silicon surface. At high etching current density more than 60mA/cm2) XRD spectra showed that the structure is amorphous.

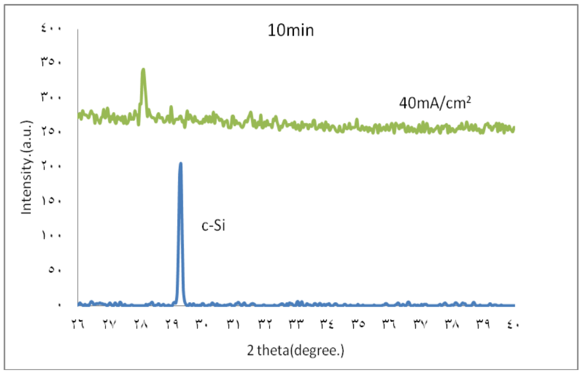

Fig. 6: XRD spectra of c-Si and PS samples anodized for 10 min etching time, 40mAcm^{-2} etching current density.

X-ray diffraction pattern can clearly display the crystal composition and structure. A broad reflection indicates that its average crystal size is smaller than that of in the crystalline silicon according to the Scherrer equation [19]:

$$L = 0.9\lambda / B\cos(\theta) \qquad (3)$$

where λ is the wavelength of the incident X-rays (0.15406 nm), B is the half value breadth of the diffracted beam and θ is the Bragg angle. Thus, it was possible to estimate an average crystal size, (L). The results indicate that the average crystal sizes are in the nanometer range [20]. The increase in lattice constant than that of the substrate has also been observed in porous silicon and suggested that the increase in lattice constant arises from stress induced by growth of a native oxide on the surface on the pore structures [21]. From the figure showing that in spite of its porosity, a PS layer remains a nearly perfect single crystal. The presence of this peak in all the PS structure confirms that the cubic structure of the crystalline silicon is retained even after the pore formation. The strain $\Delta a/a \sim 10^{-4}$, the origin of this expansion is related to the hydrogen-silicon bonds at the inner surface of the PS layer and that agreement with Bomchil et al. [22] reported $\Delta a/a = 4 \times 10^{-3}$ and 10^{-3} for p− and p+ samples of 56% and 72% porosities respectively. The increase crystallite size related by the wafer Si but with increase etching time PS increasing as we shown in Table2.

Table2: XRD parameters results for porous silicon n-type at 40 mAcm^{-2} current density

n-Type **J=40 mAcm^{-2}**	Time anodized min	2theta degree	d A	FWHM Rad.	Crystalline Size L nm	Lattice constant a nm	Strain $\Delta a/a$ %	hkl
λ=1.540 A	0	29.38	3.036	0.116	128.7	5.25	0.000313	111
a=5.43 A **K=0.9**	10	28.86	3.09	0.172	159.5	5.35	0.000177	111

5. Morphology Study

Fig.7 reveals that the formation current density plays a significant role in controlling porous morphology which is considered as a very important feature for many applications [23]. At 20in homogeneous structure and rough surface as shown in Figure (4-A1).increasing the current density produces more uniform porous layer.

Fig.7 shows that the porous morphology formation has been confirmed using optical microscopy investigation .It is observed that current density plays a significant role in controlling porous morphology. After etching, at all current densities, the porous surface shows different colors between golden and yellow, also some time close to red resulting may be sub oxide of silicon . This confirms the anodic dissolution of the silicon surface leading to porous structure formation and the visual observation of the silicon surface is considered as a very important feature gave photoluminescence. Photoluminescence in simple terms is a reverse process of absorption, so the different color resulting from broadening of the band gap energy occurs when there is a decrease in the crystallite size.

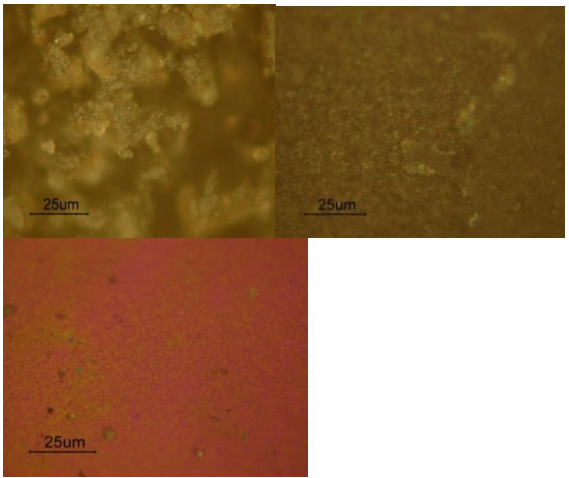

A1. J=20 A2. J=40 A3. J=60mAcm^{-2}

Fig.7: A1, A2 and A3 optical micrograph of PS surface on n-Si formed at different current densities (M=1000).

Increasing the current density to 40 and 60 mAcm^{-2} produces more uniform porous layer and small wall width between pore could be observed in this case as shown in Fig.4 (A2 and A3). From Fig.8, optical micrograph shows that the distinct variation between the fresh silicon surface and the porous silicon surfaces formed at 40mA/cm^2 etching current density for 10 min etching time.

Conclusions

Structural and morphological properties of n-type porous silicon synthesized by electrochemical etching with aid of laser are investigated. XRD and FTIR analysis confirmed the formation of porous structure. The properties of porous silicon are found strongly dependence on etching current.

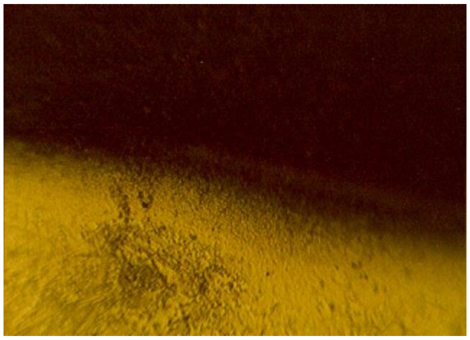

Fig.8: Optical images of cross-sections of porous silicon PS/Si –interface

References

1. M.Jayachandran, M.Paramasivam, K.R.Murali, D.C.Trivedi M.Raghavan, Meter. Phys. Mech., 4 (2001) 143-147.
2. Pap, Andrea Edit, "Investigation of pristine and oxidized porous silicon, Faculty of Technology," Ph.D.Thesis. University of Oulu.Finland. (2005).
3. J.P. Kar, S. K.Mothanta, G. Bose, S.Tuli, A.Kamra, V. Mathur, Journal of Optoelectronic and Advanced Material, 11, 3 (2009) 238–242.
4. P.M. Fauchet, IEEE J. Select. Topics in Quantum Electron, 4 (1998) 1020.
5. A. Prasad, S. Balakrishnan, S.K. Jain, and G.C. Jain , J. Electrochem. Soc., 129 (1982) 596.
6. A. JR. Uhlir, The Bell System Technical Journal, 35 (1956) 333-347.
7. S. L. Zhang, F. M. Huang, K. S. Ho, L. Jia, C. L. Yang, J.J. Li, T. Zhu, Y. Chen, S. M. Cai, A. Fujishima , Z. F. Liu, Phys. Rev., B 51 (1995) 16.
8. L. T. Canham, J. Phys. Chem. Solids, 47 (1986) 363.
9. J.P. Kar, S. K.Mothanta, G. Bose, S.Tuli, A.Kamra, V. Mathur, Journal of Optoelectronic and Advanced Material, 11,3 (2009) 238 – 242.
10. L. T. Canham, “Properties of porous silicon” Inspect, England, (1998).
11. V.Lehmann, and U.Gösele, Applied Physics Letters, 58 (1991) 856-858.
12. P. C. Searson, J. M. Macaulay, and F. M. Ross, Journal of Applied Physics 72 (1992) 253-258.
13. O.Bisi, S.Ossicini, L.Pavesi, Surface Science Reports 38, 1 (2000) 126.
14. J. Michael, “Porous Silicon in Practice: Preparation, Characterization and Applications,” First Edition by Wiley-VCH Verlag GmbH & Co. KGaA, (2012) ,p15.
15. P.M. Fauchet, L. Tsybescov, S.P. Duttagupta, K. D.Hirshmann, Thin Solid Films, 297, 1-2 (1997) 254-260.
16. M.Q. Zayer, "Studying the Effects of Annealing Process on the Structural, Optical and Electrical Properties of Porous Silicon," M.Sc. Thesis University of Technology Applied Sciences, 2010.
17. H.Li, Electrochemical and Solid State Letters, 2,11 (1999) 547-549
18. H.Foll, M.Chistophersen, J. Carstensen, G. Hasse, Materials Science and Engeering, R 39(2002) 93-141.
19. K. Omar, A. Ramizy, and Z. Hassan, Superlattices and Microstructures 50 (2011) 119–127
20. M.Q. Zayer, "Studying the Effects of Annealing Process on the Structural, Optical and Electrical Properties of Porous Silicon," M.Sc. Thesis University of Technology Applied Sciences, (2010).
21. I.M.Young, M.I.Beale, J.D.Benjamin, Appl.Phys. Lett., 46, (1985) 1133
22. G. Bomchil, A. Halimaoui, and R. Herino, Microelectronic Engineering, 8 (1988) 293.
23. M.A. Al-Jaafar, "Production of Porous Silicon and Studying Its Electrical Properties," M.Sc.Thesis.University of Technology, Iraq (2007).